IEEE Access
Multidisciplinary ⋮ Rapid Review ⋮ Open Access Journal

Received November 28, 2021, accepted December 27, 2021, date of publication December 30, 2021,
date of current version January 5, 2022.

Digital Object Identifier 10.1109/ACCESS.2021.3139324

Wideband Three-Port Equilateral Triangular Patch Antenna Generating Three Uncorrelated Waves for 5G MIMO Access Points

KIN-LU WONG, (Fellow, IEEE), AND GUAN-LIN YAN, (Student Member, IEEE)
Department of Electrical Engineering, National Sun Yat-sen University, Kaohsiung 80424, Taiwan

Corresponding author: Kin-Lu Wong (wongkl@mail.nsysu.edu.tw)

This work was supported by the Ministry of Science and Technology, Taiwan, under Grant MOST 110-2224-E-110-001 and Grant MOST 108-2221-E-110-005.

ABSTRACT A wideband three-port equilateral triangular (ET) patch antenna capable of generating three uncorrelated broadside-radiation waves for 5G MIMO access-point application is presented. The three-port ET patch antenna has a simple structure for easy implementation. To our best knowledge, using a simple ET patch antenna to generate three uncorrelated waves for MIMO application is reported for the first time. The ET patch is mounted 11.5 mm above the ground plane and has three L-strip capacitive feeds placed below the patch's three triangular tips. Three isolated fundamental TM_{10} modes polarized in three different directions can be excited to generate three uncorrelated waves at the same time. With a patch length of only 38 mm (0.48λ at 3.75 GHz), the three-port ET patch antenna covers 3.3-4.2 GHz (5G N77 band) with impedance matching <-10 dB and port isolation >15 dB. Details of the three-port ET patch antenna are presented.

INDEX TERMS Three-port single-patch antennas, equilateral triangular patch antennas, MIMO antennas, 5G antennas, MIMO access-point antennas.

I. INTRODUCTION

The wideband three-port patch antenna capable of generating three uncorrelated broadside-radiation waves has recently been reported for 5G mobile communication applications [1]–[3]. Such wideband three-port antennas are applicable as a building unit to achieve compact multi-input multi-output (MIMO) antenna arrays for outdoor base stations [1], [2] or indoor access points [3]. To achieve wideband operation in [1], two superimposed Y-shaped structures of different frequencies are used to obtain a fractional bandwidth of about 20%. Additionally, the antenna structure in [1], [2] is an all-metal structure with no substrate materials used, which is an advantage for practical applications to avoid substrate issues, such as the substrate's ohmic losses and tolerance. In [3], the wideband circular patch antenna with three probe feeds spaced by 120° can generate three isolated TM_{11} modes [4] to cover 3.3-4.2 GHz (5G N77 band) [5].

Note that, different from generating three uncorrelated broadside-radiation waves in [1]–[3], there are also three-port single-patch antennas reported to obtain three uncorrelated waves, such as generating three uncorrelated monopolar-like waves [6] or exciting two broadside-radiation waves plus one monopole-like wave [7]–[11] or achieving three directional quasi-Yagi waves with pattern diversity [12]. Most of the reported three-port patch antennas [3], [6]–[12] include using substrate materials in implementing the antennas. With an all-metal structure to avoid the substrate issues as shown in [1], [2], the multi-port patch antenna will be more attractive for practical MIMO antenna applications.

In this study, we present a wideband three-port equilateral triangular (ET) patch antenna to generate three uncorrelated broadside-radiation waves over a wide band of 3.3-4.2 GHz for 5G MIMO access-point application. The proposed antenna uses a simple ET patch and three L-strip capacitive feeds spaced by 120° below the patch to generate three isolated fundamental modes (TM_{10} modes [13]). Three broadside-radiation waves polarized in three different directions can be generated in the proposed antenna.

In addition, very low envelope correlation coefficients (ECC $<$ 0.01) between the three generated waves are obtained in the desired wide band. Also, except that the ET patch is supported by a plastic post above the ground plane,

The associate editor coordinating the review of this manuscript and approving it for publication was Young Jin Chun.

the proposed antenna is with an all-metal antenna structure to avoid the substrate issues [1], [2].

It is also noted that there have been many ET patch antennas reported in the open literature, to name a few in [13]–[19]. Very few of the reported ET patch antennas are for MIMO operation. In [19], the use of three separate ET patch antennas to generate three broadside-radiation waves for MIMO operation has been studied. However, since three separate ET patches are used, the total size of the three-port MIMO antenna is greatly increased [19]. It is to our best knowledge that using a simple ET patch antenna to generate three uncorrelated waves for MIMO application is reported in this work for the first time.

Additionally, by covering 3.3-4.2 GHz for 5G wideband MIMO application, the ET patch in the proposed antenna requires a patch length of only 38 mm (0.48λ at 3.75 GHz), similar to the conventional half-wavelength ET patch antenna operated in the fundamental TM_{10} mode [13]. That is, with three uncorrelated waves obtained at the same time, the proposed three-port ET patch antenna has a similar size as the conventional ET patch antenna. Details of the three-port ET patch antenna are presented.

II. THREE-PORT EQUILATERAL TRIANGULAR PATCH ANTENNA

Fig. 1 shows the proposed wideband three-port ET patch antenna for 5G MIMO access-point application. To cover the wide band of 3.3-4.2 GHz (5G N77 band), the ET patch with a length of 38 mm (0.48λ at 3.75 GHz) is mounted 11.5 mm above the ground plane. That is, the antenna has an air substrate of thickness 11.5 mm. Three capacitive L-strip feeds (Ports 1-3) are placed 3.3 mm below the three tips of the ET patch and all face toward the patch center. Through the 3.3 mm coupling gap, each L-strip feed capacitively excite the TM_{10} mode of the ET patch antenna [13]. In the study, the ET patch, L-strip feeds, and ground plane all use a 0.2 mm thick copper plate.

Each L-strip feed has a horizontal plate of 9×9 mm^2 and a vertical plate of 7×7 mm^2. The horizontal plate size can be varied to adjust the capacitive coupling for the TM_{10} mode excitation. The width of the vertical plate can be varied to finely adjust the inductive reactance seen from each port. The selected dimensions of the L-strip feeds in the proposed antenna can excite three isolated TM_{10} modes with the reflection coefficients ($S_{11} = S_{22} = S_{33}$, owing to symmetric structure of the antenna) lower than −10 dB and the transmission coefficients ($S_{12} = S_{13} = S_{23}$) lower than −15 dB in 3.3-4.2 GHz as shown in Fig. 2. The minimum value of the transmission coefficients is only about −32 dB at 3.65 GHz, which also occurs near the frequency with the lowest reflection coefficient. The simulated S parameters shown in Fig. 2 are obtained from the commercially available HFSS simulation tool [20].

In Fig. 2, the S_{11} of the single-port case (Port 1 only, Ports 2 and 3 not present) is also shown for comparison. It is seen that the S_{11} of the proposed three-port case and single-port case is almost the same. This indicates that the presence of Ports 2 and 3 has very small effects on the excited TM_{10} mode of Port 1. This can confirm that the

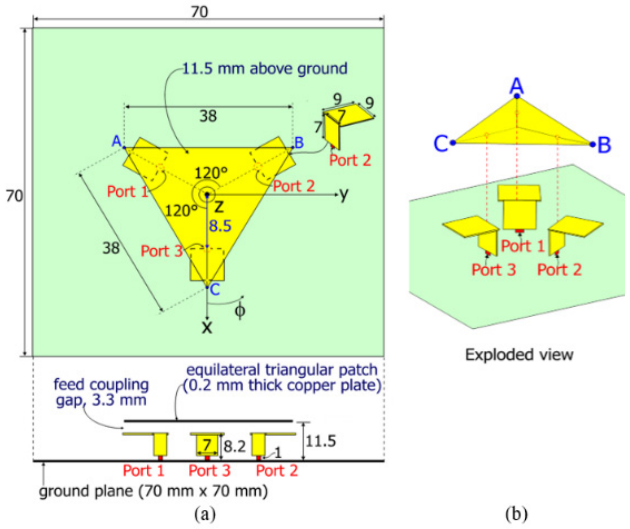

FIGURE 1. Wideband three-port ET patch antenna for 5G MIMO access points. (a) Top and side views. (b) Exploded view.

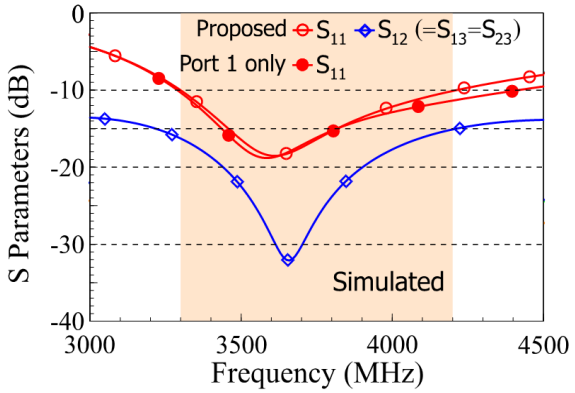

FIGURE 2. Simulated S parameters of the 3-port ET patch antenna and the single-port case (Port 1 only).

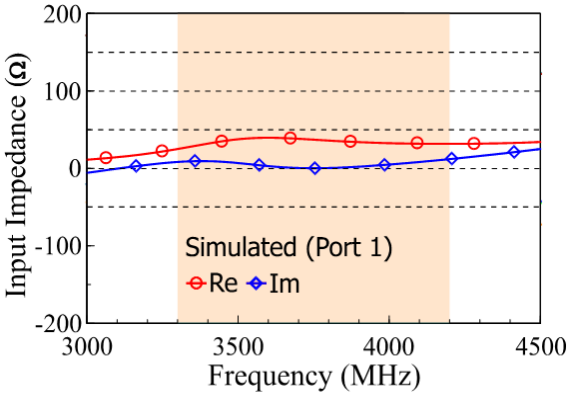

FIGURE 3. Simulated input impedance of Port 1 in the 3-port ET patch antenna.

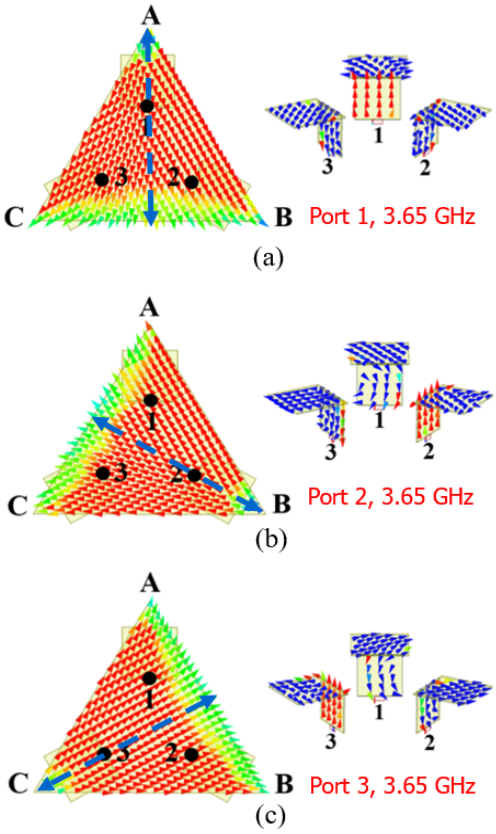

FIGURE 4. Simulated vector surface current distributions on the ET patch and feed strips at 3.65 GHz. (a) Port 1. (b) Port 2. (c) Port 3.

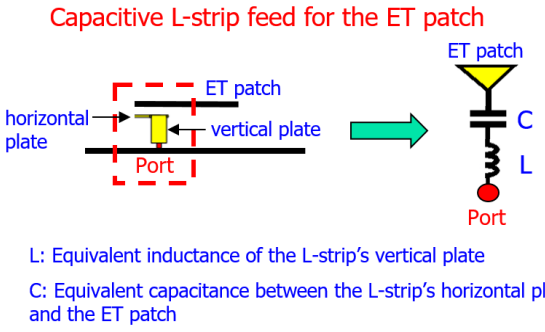

FIGURE 5. Equivalent circuit of the coupling L-strip feed for the ET patch in the study (assuming for the single-port case).

three TM_{10} modes excited in the three-port ET patch antenna can be considered to be isolated to each other.

Fig. 3 shows the input impedance seen at Port 1 of the three-port ET patch antenna. It is seen that both the real and imaginary parts of the input impedance are varied slowly in 3.3-4.2 GHz. In addition, the imaginary part or the input reactance is close to zero. The impedance characteristic confirms that the L-strip capacitive feeds can lead to good impedance matching of the TM_{10} mode excitation over a wide operating band in this study.

The simulated vector surface current distributions on the ET patch and feed strips at 3.65 GHz for Ports 1-3 are also shown in Fig. 4. For Port 1 excitation in Fig. 4(a), the surface currents indicate that the excited TM_{10} mode is mainly resonant from Point A toward its opposite edge BC. Similarly, for Port 2 excitation in Fig. 4(b), it indicates that the excited TM_{10} mode is mainly resonant from Point B toward its opposite edge AC. Similarly, for Port 3 shown in Fig. 4(c), the TM_{10} mode is excited and resonant from Point C toward its opposite edge AB. The results indicate that the three excited TM_{10} modes are resonant in three different directions. This can lead to very low correlation of the three generated waves, which will be further discussed later in the next section. Also, the surface currents on the feed strips confirm good port isolation of Ports 1-3.

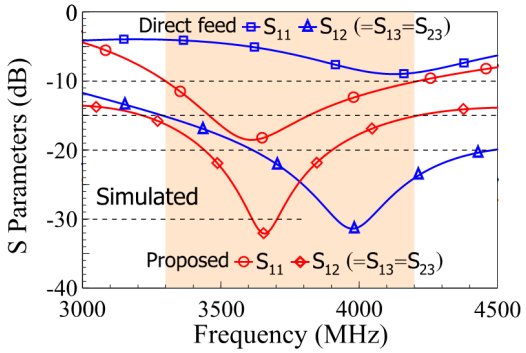

FIGURE 6. Simulated S parameters of the 3-port ET patch antenna with L-strip feeds and direct feeds (no coupling gap).

To explain the coupling mechanism of the capacitive L-strip feed in the proposed antenna, Fig. 5 shows an equivalent circuit of the L-strip feed which consists of a series inductance L and a series capacitance C. The single-port case for the antenna is considered for simplicity. The series inductance L can be adjusted by the L-strip's vertical plate (size selected to 7×7 mm^2 here), whose equivalent inductance can be evaluated with the aid of the flat wire inductor calculator [21].

On the other hand, the series capacitance C is a function of the L-strip's horizontal plate (size selected to 9×9 mm^2 here) and the coupling gap (selected to 3.3 mm here) between the L-strip and the ET patch. By adjusting the equivalent series inductance and capacitance of the L-strip feed, smooth variation of the input impedance over a wide operating band is obtained as shown in Fig. 3.

Fig. 6 shows a comparison of the simulated S parameters of the 3-port ET patch antenna with L-strip feeds (proposed) and direct feeds. In the direct-feed case, the feed strip has the vertical plate only (size selected to 7×11.5 mm^2) and is directly connected to the ET patch. Results show that the impedance matching is very poor (larger than -9 dB) over the desired wide band for the direct-feed case. The poor impedance matching is mainly owing to the excess equivalent inductance of the feed strip, although the feed strip has a wide strip width of 7 mm to decrease its equivalent inductance.

On the other hand, with the additional capacitance contributed by the equivalent series capacitance shown in Fig. 5

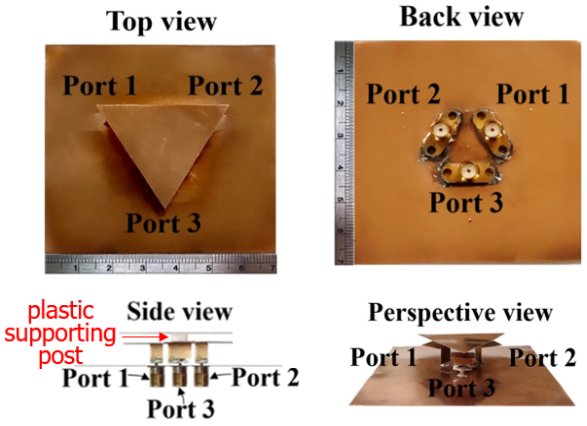

FIGURE 7. Fabricated three-port ET patch antenna.

for the L-strip feed, much better impedance matching over a wide band for the proposed antenna is obtained.

III. EXPERIMENTAL RESULTS AND DISCUSSION

Fig. 7 shows the fabricated three-port ET patch antenna. In the experiment, the ET patch is supported above the ground plane using a plastic post placed between the patch center and the ground plane. To excite the antenna, the three L-strip feeds with Ports 1-3 are connected to three SMA connectors on the back side of the ground plane.

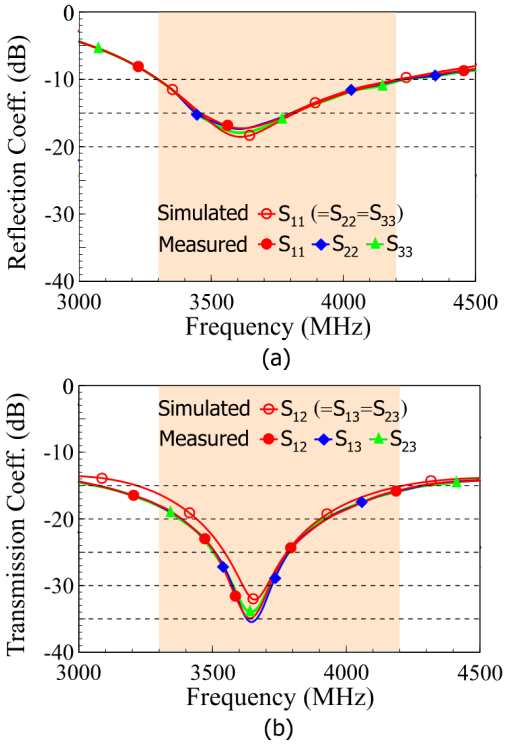

FIGURE 8. Measured (a) reflection and (b) transmission coefficients of the fabricated antenna. Simulated results of Port 1 are shown for comparison.

Fig. 8 shows the measured *S* parameters of the fabricated antenna. Fig. 8(a) shows the measured reflection coefficients

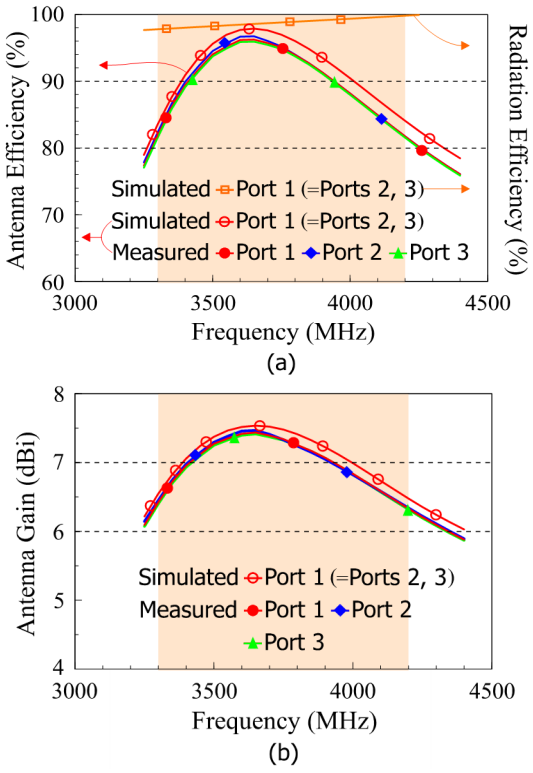

FIGURE 9. Measured (a) antenna efficiency and (b) antenna gain of Ports 1-3. Simulated results of Port 1 are shown for comparison.

of Ports 1-3. Fig. 8(b) shows the measured transmission coefficients. The simulated *S* parameters of Port 1 are included in the figure for comparison. Good agreement of the measurement and simulation is obtained. In the wide band of 3.3-4.2 GHz, the measured reflection coefficients are less than −10 dB and the measured transmission coefficients are less than −15 dB. Also note that at about 3.65 GHz where the minimum reflection coefficient occurs, the measured transmission coefficient is only about −35 dB.

The measured antenna efficiency and antenna gain are respectively shown in Fig. 9(a) and (b). Note that in Fig. 9(a), the presented antenna efficiency includes the mismatching loss and is the total efficiency. For comparison, the radiation efficiency for perfect matching condition is also included in the figure, which is larger than 97% in 3.3-4.2 GHz. The measured results also agree with the simulation prediction. The measurement is conducted in a far-field anechoic chamber and calibrated using a standard horn antenna. The measured antenna efficiency is larger than 82% and the measured antenna gain is about 6.3-7.4 dBi in 3.3-4.2 GHz.

The radiation patterns of Ports 1-3 are also measured. With the measured three-dimensional (3-D) radiation patterns [22], the ECC of the three generated waves is calculated, which is shown in Fig. 10. The calculated ECC is lower than 0.01 in 3.3-4.2 GHz. This indicates that the three generated waves can be considered to be uncorrelated. The HFSS simulated ECC shown in the figure is also very low and confirms

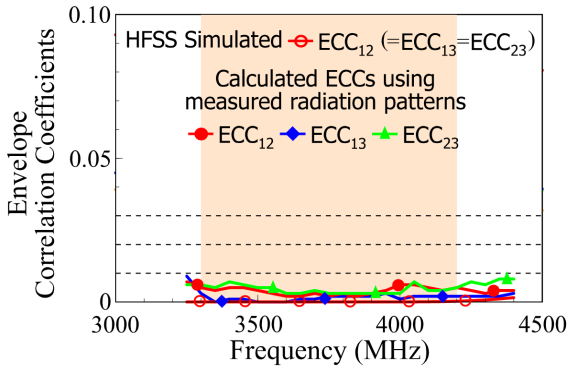

FIGURE 10. Calculated ECC based on the measured radiation patterns and HFSS simulated ECC.

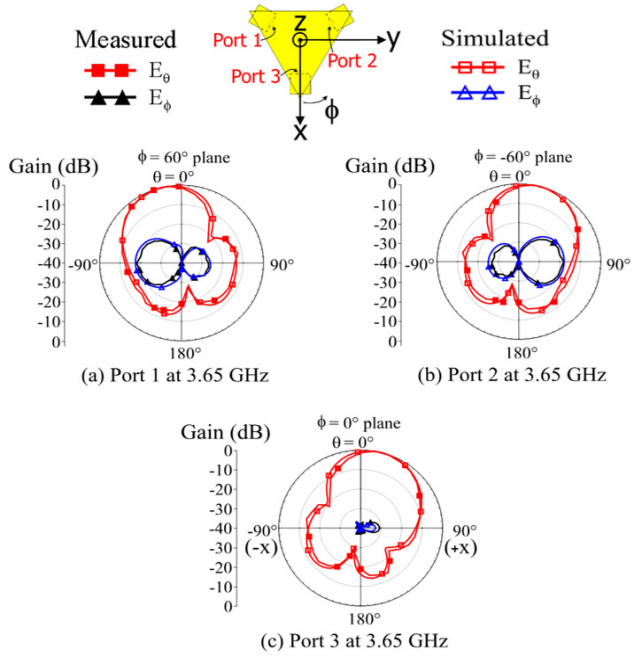

FIGURE 11. Measured and simulated radiation patterns at 3.65 GHz. (a) Port 1, $\phi = 60°$ plane. (b) Port 2, $\phi = -60°$ plane. (c) Port 3, $\phi = 0°$ plane.

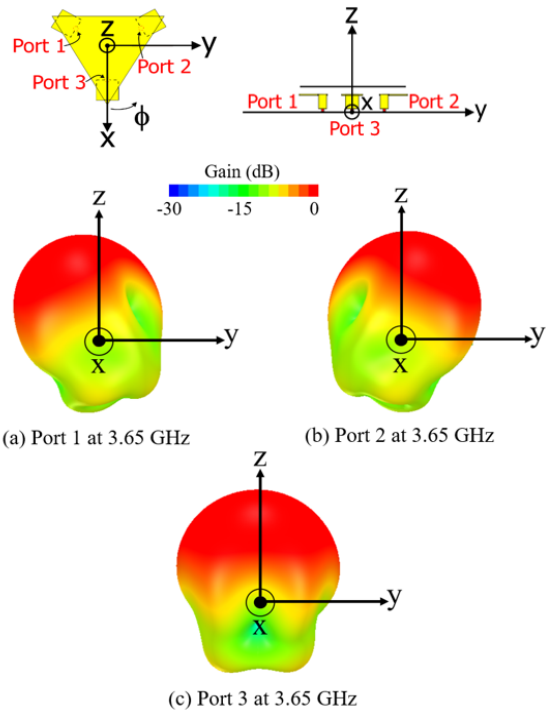

FIGURE 12. Simulated 3-D total-power radiation patterns at 3.65 GHz. (a) Port 1. (b) Port 2. (c) Port 3.

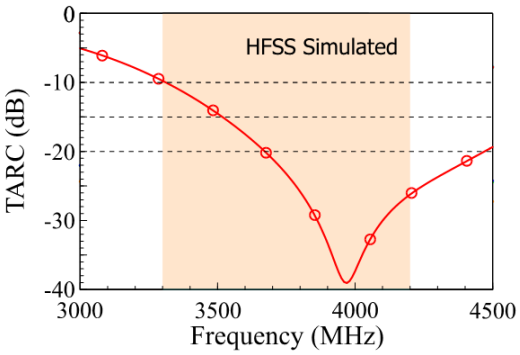

FIGURE 13. Simulated total active reflection coefficient (TARC) for the 3-port ET patch antenna.

that three uncorrelated waves are generated in the proposed antenna.

Note that the ECC results shown in Fig. 10 are obtained based on the rigorous 3-D far-field radiation patterns with an expression given in [22]. The calculated ECC uses the measured amplitude and phase of the respective far-field electric fields excited by Ports 1-3 of the antenna. On the other hand, the HFSS [20] simulated ECC uses the simulated amplitude and phase of the far-field electric fields of Ports 1-3. The ECC_{12} in the figure indicates the correlation between the two waves generated by Ports 1 and 2. Similarly, the ECC_{13} is the correlation of the generated waves of Port 1 and 3, while the ECC_{23} is the corresponding result related to Ports 2 and 3.

The measured and simulated two-dimensional (2-D) radiation patterns of Ports 1-3 at 3.65 GHz are shown in Fig. 11. The radiation patterns in the $\phi = 60°$ plane for Port 1, in the $\phi = -60°$ plane for Port 2, and in the $\phi = 0°$ plane for Port 3 are respectively plotted in Fig. 11(a), (b), and (c). Broadside or near-broadside radiation is seen. The measured and simulated results are seen in agreement. For Port 1, its generated wave is slightly tilted away from the patch center (the z-axis) to the direction of Port 1. Similar characteristic is also seen for the generated waves of Ports 2 and 3. This characteristic can be seen clearer from the corresponding HFSS simulated 3-D total-power radiation patterns at 3.65 GHz for Ports 1-3 shown in Fig. 12. Since the three generated waves are polarized in three different directions and also slightly tilted away respectively from the z-axis to Ports 1-3, which may account for the very low ECC obtained in Fig. 10.

The HFSS [20] sim ion coefficient (TARC) [22], [23] for the proposed MIMO antenna is also presented in Fig. 13.

The TARC results are obtained by considering that Ports 1-3 of the antenna are all excited with unity amplitude and same phases for transmitting three synchronized MIMO signals. In the operating bandwidth of interest (3.3-4.2 GHz), the TARC is seen to be less than −10 dB.

IV. CONCLUSION

The wideband three-port ET patch antenna for 5G MIMO access-point application has been proposed and studied. With a simple structure and a patch length of only 38 mm (0.48λ at 3.75 GHz), the antenna can generate three uncorrelated broadside or near-broadside waves with very low ECC (<0.01) over the wide band of 3.3-4.2 GHz (5G N77 band). Details of the antenna structure and operating principle have been addressed. The experimental results of the fabricated antenna also verify the simulation prediction. The three-port ET antenna will be promising for indoor MIMO access-point applications.

REFERENCES

[1] C.-Y. Chiu, B. K. Lau, and R. Murch, "Bandwidth enhancement technique for broadside tri-modal patch antenna," *IEEE Open J. Antennas Propag.*, vol. 1, pp. 524–533, 2020.
[2] C.-Y. Chiu, S. Shen, B. K. Lau, and R. Murch, "The design of a trimodal broadside antenna element for compact massive MIMO arrays: Utilizing the theory of characteristic modes," *IEEE Antennas Propag. Mag.*, vol. 62, no. 6, pp. 46–61, Dec. 2020.
[3] K.-L. Wong, C.-M. Chou, Y.-J. Yang, and K.-Y. Wang, "Multipolarized wideband circular patch antenna for fifth-generation multi-input–multi-output access-point application," *IEEE Antennas Wireless Propag. Lett.*, vol. 18, no. 10, pp. 2184–2188, Oct. 2019.
[4] K. L. Wong, *Compact and Broadband Microstrip Antennas*. New York, NY, USA: Wiley, 2002.
[5] White Paper of GSA (The Global mobile Suppliers Association). (Jan. 4, 2020). *3300–4200 MHz: A key frequency band for 5G*. [Online]. Available: https://gsacom.com/paper/3300-4200-mhz-a-key-frequency-band-for-5g/
[6] K.-L. Wong, H.-J. Chang, J.-Z. Chen, and K.-Y. Wang, "Three wideband monopolar patch antennas in a Y-Shape structure for 5G multi-input–multi-output access points," *IEEE Antennas Wireless Propag. Lett.*, vol. 19, no. 3, pp. 393–397, Mar. 2020.
[7] S. X. Ta, D. M. Nguyen, K. K. Nguyen, C. Dao-Ngoc, and N. Nguyen-Trong, "A tripolarized antenna with ultrawide operational bandwidth," *IEEE Trans. Antennas Propag.*, vol. 68, no. 6, pp. 4386–4396, Jun. 2020.
[8] D. Piao and Y. Wang, "Tripolarized MIMO antenna using a compact single-layer Microstrip patch," *IEEE Trans. Antennas Propag.*, vol. 67, no. 3, pp. 1937–1940, Mar. 2019.
[9] Y. Zhang, K. Wei, Z. Zhang, and Z. Feng, "A broadband patch antenna with tripolarization using quasi-cross-slot and capacitive coupling feed," *IEEE Antennas Wireless Propag. Lett.*, vol. 12, pp. 832–835, 2013.
[10] X. Gao, H. Zhong, Z. Zhang, Z. Feng, and M. F. Iskander, "Low-profile planar tripolarization antenna for WLAN communications," *IEEE Antennas Wireless Propag. Lett.*, vol. 9, pp. 83–86, 2010.
[11] H. Zhong, Z. Zhang, W. Chen, Z. Feng, and M. F. Iskander, "A tripolarization antenna fed by proximity coupling and probe," *IEEE Antennas Wireless Propag. Lett.*, vol. 8, pp. 465–467, 2009.
[12] Y. Xu, Y. Dong, S. Wen, and H. Wang, "Vertically polarized quasi-yagi MIMO antenna for 5G N78 band application," *IEEE Access*, vol. 9, pp. 7836–7844, 2021.
[13] K.-F. Lee, K. Luk, and J. S. Dahele, "Characteristics of the equilateral triangular patch antenna," *IEEE Trans. Antennas Propag.*, vol. AP-36, no. 11, pp. 1510–1518, Nov. 1988.
[14] X. Deng, X. Xu, and Y. Wang, "Design of an S-Band equilateral triangular patch antenna (ETPA) on mushroom metamaterials in compact configuration," in *Proc. 12th Int. Symp. Antennas, Propag. EM Theory (ISAPE)*, Dec. 2018, pp. 1–2.
[15] B. Singh, N. Sarwade, and K. P. Ray, "A 50-Ω microstrip line fed shorted equilateral triangular microstrip antenna," *Microw. Opt. Technol. Lett.*, vol. 60, no. 5, pp. 1219–1222, May 2018.
[16] C.-L. Tang and K.-L. Wong, "A modified equilateral-triangular-ring microstrip antenna for circular polarization," *Microw. Opt. Technol. Lett.*, vol. 23, no. 2, pp. 123–126, Oct. 1999.
[17] J.-H. Lu, C.-L. Tang, and K.-L. Wong, "Novel dual-frequency and broadband designs of slot-loaded equilateral triangular microstrip antennas," *IEEE Trans. Antennas Propag.*, vol. 48, no. 7, pp. 1048–1054, Jul. 2000.
[18] J.-H. Lu and K.-L. Wong, "Single-feed circularly polarized equilateral-triangular microstrip antenna with a tuning stub," *IEEE Trans. Antennas Propag.*, vol. 48, no. 12, pp. 1869–1872, Dec. 2000.
[19] H. Zhang, Z. Wang, J. Yu, and J. Huang, "A compact MIMO antenna for wireless communication," *IEEE Antennas Propag. Mag.*, vol. 50, pp. 104–107, Dec. 2008.
[20] (2018). *ANSYS HFSS*. (Oct. 1, 2018). [Online]. Available: http://www.ansys.com/staticassets/ ANSYS/staticassets/resourcelibrary/brochure/ansys-hfss-brochure-19.1. pdf
[21] (Jul. 1, 2021). *Flat Wire Inductor Calculator, Chemandy Electronics*. [Online]. Available: https://chemandy.com/calculators/flat-wire- inductor-calculator.htm
[22] M. S. Sharawi, "Printed multi-band MIMO antenna systems and their performance metrics," *IEEE Antennas Propag. Mag.*, vol. 55, no. 5, pp. 218–232, Oct. 2013.
[23] M. Manteghi and Y. Rahmat-Samii, "Multiport characteristics of a wideband cavity backed annular patch antenna for multipolarization operations," *IEEE Trans. Antennas Propag.*, vol. 53, no. 1, pp. 466–474, Jan. 2005.

KIN-LU WONG (Fellow, IEEE) received the B.S. degree in electrical engineering from the National Taiwan University, Taipei, Taiwan, in 1981, and the M.S. and Ph.D. degrees in electrical engineering from Texas Tech University, Lubbock, TX, USA, in 1984 and 1986, respectively.

From 1986 to 1987, he was a Visiting Scientist with the Max Planck Institute for Plasma Physics, Munich, Germany. Since 1987, he has been with the Department of Electrical Engineering, National Sun Yat-sen University (NSYSU), Kaohsiung, Taiwan, where he became a Professor, in 1991. From 1998 to 1999, he was a Visiting Scholar with the Electroscience Laboratory, The Ohio State University, Columbus, OH, USA. He was elected to be the Sun Yat-sen Chair Professor at NSYSU, in 2005, the Distinguished Chair Professor of NSYSU, in 2017, and the National Chair Professor of the Ministry of Education, Taiwan, in 2016. He was also the Chairperson of the Department of Electrical Engineering, NSYSU, from 1994 to 1997, the Vice President for Research Affairs, from 2005 to 2007, and a Senior Vice President of NSYSU, from 2007 to 2012. He is currently the National Chair Professor of the Ministry of Education, a Distinguished Researcher of the Ministry of Science and Technology, and the Distinguished Chair Professor of the National Sun Yat-sen University, a Thomson Reuters Highly Cited Researcher, and an Elsevier Most Cited Researcher. He was elected as a Thomson Reuters Highly Cited Researcher, in 2014 and 2015, and an Elsevier Most Cited Researcher, in 2015. In 2008, the research achievements on handheld device antennas at the NSYSU Antenna Laboratory led by him was selected to be top 50 scientific achievements of Taiwan Ministry of Science and Technology in past 50 years, from 1959 to 2009. He has authored more than 580 refereed journal articles and 300 conference papers. He has personally supervised 57 graduated Ph.D. students. He holds over 300 patents, including over 100 U.S. patents. He is the author of *Design of Nonplanar Microstrip Antennas and Transmission Lines* (Wiley, 1999), *Compact and Broadband Microstrip Antennas* (Wiley, 2002), and *Planar Antennas for Wireless Communications* (Wiley, 2003). His published articles have been cited over 33,000 times with an H-index of 86 in Google Scholar.

Dr. Wong was a recipient of the 2010 Outstanding Research Award from the Pan Wen Yuan Foundation and selected as a top 100 honor of Taiwan by global views monthly in August 2010 for his contribution in mobile antenna researches. He was also a recipient of the Academic Award from the Taiwan Ministry of Education, in 2012, the Outstanding Distinguished Researcher Award from the Taiwan Ministry of Science and Technology, in 2013, the Outstanding Research Award three times from the Taiwan National Science Council, in 1995, 2000, and 2002, the Outstanding Electrical Engineering Professor Award from the Institute of Electrical Engineers of Taiwan, in 2003, and the Outstanding Engineering Professor Award from the Institute of Engineers of Taiwan, in 2004. He was awarded the Best Associate Editor two times for the IEEE TRANSACTIONS ON ANTENNAS AND PROPAGATION, in 2015 and 2016. He and his graduate students have been awarded the Best Paper Award (APMC Prize) in 2008 APMC, and the Best Student Paper Award/Young Scientist Award in 2007 ISAP, 2008 APMC, 2009 ISAP, 2010 ISAP, 2012 ISAP, and 2016 ISAP. His graduate students also won the first prize from the Taiwan National Mobile Handset Antenna Design Competition, in 2007 and 2009. He served or serves as an IEEE AP-S AdCom Member, an IEEE AP-S Transactions Track Editor/Associate Editor, an AP-S Transactions Paper Awards Committee Member, and an AP-S Field Awards Committee Member. He was also a PE7 Panel Member of 2015, 2017, and 2019 European Research Council Advanced Grant Panel and the Chief Consultant of the Institute of Antenna Engineers of Taiwan. He served as the Chair of the judge panel for the National Communication Antenna Design Competition organized by Taiwan Ministry of Economics, from 2014 to 2021. He has been an international steering committee member for many international conferences. He served as the General Chair for 2012 APMC, 2014 ISAP, and 2016 APCAP, Kaohsiung.

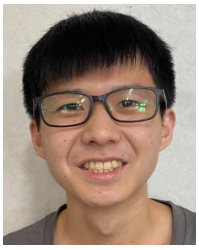

GUAN-LIN YAN (Student Member, IEEE) received the B.S. degree in electrical engineering from the National Pingtung University, Pingtung, Taiwan, in 2020. He is currently pursuing the M.S. degree with the National Sun Yat-sen University, Kaohsiung, Taiwan. His main research interests include MIMO antennas for 5G mobile-device and access-point applications.